Title
Force-Based Design Method for Force-Limiting Deformable Connections in Earthquake-Resistant Buildings

Journal
Journal of Structural Engineering, 148(10)

ISSN
0733-9445

Authors
Tsampras, Georgios
Sause, Richard

Publication Date
2022-10-01

DOI
10.1061/(asce)st.1943-541x.0003456

Tsampras, Georgios, Richard Sause, "Force-Based Design Method for Force-Limiting Deformable Connections in Earthquake-Resistant Buildings." Journal of Structural Engineering, 10.1061/(ASCE)ST.1943-541X.0003456

Force-based design method for force-limiting deformable connections in earthquake-resistant buildings

Georgios Tsampras, Ph.D., M.ASCE[1] and Richard Sause, Ph.D., P.E., M.ASCE[2]

[1]Assistant Professor of Structural Engineering, UC San Diego, 9500 Gilman Drive, La Jolla, CA 92093, gtsampras@ucsd.edu

[2]Joseph T. Stuart Professor of Structural Engineering, Lehigh University, 117 ATLSS/Mountaintop Drive, Bethlehem, PA 18015, rs0c@lehigh.edu

ABSTRACT

This paper proposes a force-based design method for force-limiting deformable connections that are used to transfer seismic-induced horizontal forces from the floor-diaphragms in buildings to the vertical elements of lateral seismic force-resisting systems with base flexural mechanisms (e.g., reinforced concrete shear walls). The design method determines the limiting forces for the connections at each floor of the building. The limiting forces for the connections are the forces at which the force-limiting deformable connections transition from linear-elastic to post-elastic response. The proposed design method is a modified version of the ASCE/SEI 7-16 alternative seismic design force method for floor-diaphragms. Design examples are presented. Seismic responses from numerical simulations of twelve-story, eight-story, and four-story reinforced concrete shear wall example buildings show that the proposed method enables effective preliminary design of the force-limiting deformable connections. It is shown that the buildings with connections designed with the proposed method have relatively uniform distribution of connection deformation demands over the building height. It is also shown that their seismic force and acceleration responses

have reduced magnitude and reduced variability compared to conventional buildings that exhibit large variability in their acceleration responses.

Introduction

The design of conventional earthquake-resistant building systems is associated with uncertainty in the prediction of their seismic response. This uncertainty is a result of the variability in the earthquake ground motions, and the variability in the structural characteristics and their evolution during seismic response, which in turn affects the nonlinear response of the building components (FEMA 2017; Sattar et al. 2018). More specifically, the variability in the seismic response of structural connections can be high due to the complex interactions resulting from the kinematic compatibility between structural components. For example, the interaction between the floor-diaphragms in the gravity load resisting system (GLRS) and the reinforced concrete shear wall lateral seismic force-resisting systems (LFRS) may lead to damage of the connection (Moehle et al. 2010) that results in uncontrolled transfer of forces. Because of the uncontrolled response, the seismic-induced horizontal forces in the floor-diaphragms can be large relative to the floor-diaphragm strength, and may lead to non-ductile response of the diaphragms (Fleischman and Farrow 2001). The development of excessive inertia forces due to high floor accelerations can produce nonlinear response and significant damage of the LFRS (Rodriguez et al. 2002). In addition, the peak floor accelerations can be much larger than the peak ground accelerations, when both the 1st and higher modes are fully considered in the dynamic response of buildings (Ray-Chaudhuri and Hutchinson 2011).

Review of force-limiting deformable connections in earthquake-resisting buildings

Crane 2004 conducted shake table tests on two small-scale six-story buildings with energy dissipative connections between the floors and the LFRS. Triangular-plate added damping and stiffness devices were used as the connections. Reduced floor accelerations and base overturning moment were observed.

Zhang et al. 2014 and Fleischman et al. 2015 introduced an innovative inertia force-limiting system for earthquake-resistant buildings. The innovative system uses force-limiting deformable connections between the floor-diaphragms of a flexible GLRS and the stiff vertically-oriented LFRS of an earthquake-resistant building. Fig. 1 shows a schematic example of a reinforced concrete shear wall earthquake-resistant building with force-limiting deformable connections that consist of a friction device and rubber bearings. Floor openings are introduced around the planar shear walls. The force-limiting deformable connections allow relative displacement between the floor-diaphragms and the LFRS, and transfer the seismic-induced horizontal forces from the floor-diaphragms to the LFRS. The compressive stiffness of the rubber bearings ensures the out-of-plane stability of the shear walls. The shear stiffness of the rubber bearings provides post-elastic stiffness to the deformable connections required to limit the inelastic deformation demands between the floors and the shear wall LFRS. Any vertical motion of the shear wall at each floor level is constrained only by the shear stiffness of the rubber bearings.

Tsampras et al. 2016 presented the development of the force-limiting deformable connection, where the objectives were to limit the seismic-induced horizontal forces transferred from the floor-diaphragms in buildings to the vertical elements of LFRS which have a base flexural mechanism (e.g., reinforced concrete shear walls) and to reduce the seismic-induced horizontal floor accelerations of these buildings. More specifically, the authors performed a parametric numerical study of an example twelve-story building model with force-limiting deformable connections that have idealized bilinear elastic-plastic connection force-deformation responses. The parametric study defined an approximate feasible design space for the following three properties of the force-limiting deformable connections: (1) their limiting force (i.e., the force at which each deformable connection at each floor transitions from linear-elastic to post-elastic response), (2) their linear-elastic stiffness, and (3) their post-elastic stiffness. The parametric study assumed that the force-limiting deformable connections have the same (i.e., constant) properties over the height of the building. It was concluded that a force-limiting deformable connection consisting of a friction device or a buckling-restrained brace with low damping rubber bearings can provide a combination of limiting force, linear-elastic stiffness, and post-elastic stiffness that is within the approximate feasible design space.

Tsampras and Sause 2014a, Tsampras and Sause 2014b, Tsampras et al. 2017, and Tsampras et al. 2018 presented detailed experimental studies of full-scale force-limiting deformable connections conducted at the experimental facility NHERI at Lehigh (Cao et al. 2020). Fleischman et al. 2014 and Zhang et al. 2018 discussed the shake-table experimental seismic response of a half-scale, four-story reinforced concrete flat-plate shear wall structure with force-limiting deformable connections subjected to a sequence of twenty-two ground motions simulated at the experimental facility NHERI at UC San Diego (Van Den Einde et al. 2021).

Tsampras et al. 2016 conducted numerical earthquake simulations to compare the seismic response of an example twelve-story reinforced concrete shear wall building model with experimentally calibrated force-limiting deformable connection models with the seismic response of the example building model with monolithic "rigid" (RE) connections. The RE connections had high linear-elastic stiffness compared to the stiffness of the connecting structural components and unbounded (infinite) strength. The RE connections simulated the connections between floor-diaphragms and LFRS in a conventional building. The value of the limiting force of each deformable connection at each floor of the building was the same (i.e., the connections had constant limiting force values over the height of the building) and equal to a value within the approximate feasible design space estimated in the parametric study discussed earlier. The authors concluded that the use of force-limiting deformable connections resolves the issues associated with complex interactions from kinematic compatibilities between the floor-diaphragms and the LFRS that may be difficult to accommodate with “rigid” monolithic connections. In addition, it was observed that the use of force-limiting deformable connections: (1) limits the story shear forces, floor accelerations, base shear, and forces transferred from the floor-diaphragms to the LFRS, (2) reduces the variability in the story shear forces, floor accelerations, base shear, and forces transferred from the floor-diaphragms to the LFRS due to the ground motion variability, and (3) mitigates the effects of higher mode responses on the dynamic response of the building.

The past research studies, however, also showed that the connection deformation demands depend on the numerical model of the GLRS. More specifically, Tsampras 2016 conducted numerical earthquake simulations to assess the effect of the GLRS model on the seismic response of an example twelve-story building with force-limiting deformable connections with constant limiting force over the height of the building. The results from the numerical earthquake simulations showed that reducing the stiffness of the GLRS model increases the GLRS story drift demands and the connection deformation demands without significantly affecting the LFRS story shears, GLRS story shears, connection forces, LFRS story drifts, and floor total accelerations. The building model with a pin-base lean-on column GLRS model resulted in the largest connection deformation demands. The connection deformation demands were larger at the top floors compared to the demands at the lower floors (i.e., the connection deformations were non-uniform over the height of the building).

Considering the findings from the past research studies discussed above, it is concluded that there is the need for a simple and efficient method to determine the design value of the limiting force for each deformable connection at each floor of a building. A building with force-limiting deformable connections designed using this method should have reasonable magnitudes and a relatively uniform distribution of connection deformation demands over the building height, even when a flexible pin-base lean-on column GLRS model is assumed. These buildings should have floor accelerations and seismic force responses with reduced magnitude and reduced dispersion compared to conventional buildings.

Scope of study

This paper presents: (1) a force-based design method to determine the design value of the limiting force for the force-limiting deformable connection at each floor of buildings with LFRS that have a base flexural mechanism (e.g., reinforced concrete shear wall buildings), (2) design examples, and (3) numerical simulations of twelve-story, eight-story, and four-story reinforced concrete shear wall example buildings with force-limiting deformable connections designed using the proposed method. The proposed design method is a modified version of the ASCE/SEI 7-16 (ASCE 2017) alternative seismic design force method for floor-diaphragms. The method is simple to implement in design practice. The method is also efficient since it does not require a large number of parametric numerical earthquake simulations to determine a feasible design space for the design values of the limiting force. The method provides design values for the limiting force that vary appropriately over the height of the building (e.g., larger limiting forces at the top floors compared to the lower floors of a building) by considering the relative contributions of the first and higher modes to the seismic response of the building. The design examples show design values for the limiting forces of force-limiting deformable connections for twelve-story, eight-story, and four-story reinforced concrete shear wall example buildings. Seismic responses from numerical earthquake simulations of these example buildings with force-limiting deformable connections designed using the proposed design method are compared with the seismic responses of the example buildings with deformable connections with a constant limiting force over the height of the building, and with the seismic responses of the example buildings with RE connections, which represent conventional buildings. The effect of the number of stories in the building and the magnitude of the limiting forces of the connections on the seismic response of the example buildings is studied. It is shown that the buildings with force-limiting deformable connections designed using the proposed method have a more uniform distribution of connection deformation demands over the height of the building compared to the buildings with deformable connections with constant limiting force values over the height of the building. Larger design values of the limiting force are required in the four-story building to have connection deformation demands similar to those of the eight-story and the twelve-story buildings. It is also shown that the buildings with force-limiting deformable connections designed using the proposed method have floor accelerations and force responses with reduced magnitude and dispersion compared to buildings with RE connections. The reduced magnitude and dispersion of the floor acceleration response reduces the potential for damage to acceleration sensitive nonstructural components, and reduces the uncertainty in the seismic response of the structural components of the building.

Force-based design method for force-limiting deformable connections

Review of alternative seismic design force for floor-diaphragms

As an introduction to the proposed design method, this section summarizes the calculation of the alternative seismic design force for floor-diaphragms at elevation level x denoted as F_{px} [Eq. 1], presented in FEMA P-1050 (FEMA 2015). This method was adapted by ASCE/SEI 7-16 with modifications.

$$F_{px} = \frac{C_{px}}{R_s} w_{px} \geq 0.2 S_{DS} I_e w_{px} \tag{1}$$

where C_{px} is the design acceleration coefficient at level x, R_s is the diaphragm design force reduction factor, w_{px} is the seismic weight tributary to the diaphragm at level x, S_{DS} is the design spectral acceleration at short periods, and I_e is the importance factor. The possible distributions of values of C_{px} based on the total number of floors n, are shown in Fig. 2 (FEMA 2015). The amplification of C_{px} at $h_x/h_n \geq 0.8$ for $n \geq 3$ is related to the second and higher mode contributions to the total force response. The design acceleration coefficients C_{p0} at the base and C_{pn} at the top level n are defined below:

$$C_{p0} = 0.4 S_{DS} I_e \tag{2}$$

$$C_{pn} = \sqrt{(\Gamma_{m1}\Omega_0 C_s)^2 + (\Gamma_{m2} C_{s2})^2} \tag{3}$$

$$\Gamma_{m1} = 1 + \frac{z_s}{2}(1 - \frac{1}{n}) \tag{4}$$

$$\Gamma_{m2} = 0.9 z_s (1 - \frac{1}{n})^2 \tag{5}$$

$$C_{s2} = \begin{cases} \min\left[\frac{I_e S_{D1}}{0.03(n-1)};\, (0.15n + 0.25) I_e S_{DS};\ I_e S_{DS}\right], \text{ for } n \geq 2 \\ 0, \text{ for } n = 1 \end{cases} \tag{6}$$

where Γ_{m1} is the first mode contribution factor, Ω_0 is the LFRS overstrength factor, C_s is the seismic response coefficient, Γ_{m2} is the higher mode contribution factor (assuming one contribution factor for all the modes higher than the first mode), C_{s2} is the higher mode seismic response coefficient, and z_s is the mode shape factor equal to 0.30 for buckling restrained braced frames, 0.70 for moment resisting frames, 0.85 for dual systems, and 1.00 for all other systems.

Seismic load path

This section reviews the path of seismic-induced horizontal forces in buildings with force-limiting deformable connections between the GLRS and LFRS of a building. Fig. 3 shows the seismic-induced forces acting in the GLRS and LFRS in the undeformed position of the building. For the GLRS, which is assumed to contain the majority of the seismic mass, the inertia forces due to the total acceleration are denoted $F_{I,GLRS}$, the viscous damping forces are denoted F_D, the restoring forces due to the frame action and overturning resistance of the GLRS are denoted $F_{S,GLRS}$. The forces transferred from the GLRS to the LFRS through the force-limiting deformable connections are denoted F_{DC}. For the LFRS the inertia forces due to the total acceleration are denoted $F_{I,LFRS}$, the restoring forces for the LFRS (i.e., shear wall) are denoted $F_{S,LFRS}$. For clarity, the forces in the rubber bearings and the forces developed due to the out-of-plane action of the walls are not shown in Fig. 3.

The restoring forces $F_{S,GLRS}$ and damping forces F_D of the GLRS are not zero. However, for preliminary design purposes, we assume that the seismic-induced horizontal forces are resisted entirely by the vertical elements of the LFRS, the force-limiting deformable connections, and the diaphragm. Therefore, for preliminary design, the restoring forces $F_{S,GLRS}$ and damping forces F_D of the GLRS are assumed to be negligible and $F_{I,GLRS}$ are in equilibrium with F_{DC}. In addition, if the mass associated with the shear wall is considered negligible (i.e., very small compared to the total seismic mass), F_{DC} are in equilibrium with $F_{S,LFRS}$. Thus, as a simplification for preliminary design, we can determine design values for the limiting force for each deformable connection at each floor of the building from an estimate of the inertia forces in each floor-diaphragm. In the next section the proposed force-based procedure for the design of the force-limiting deformable connections is presented.

Design values for limiting force for deformable connection at each floor

The calculations of F_{px} presented earlier, are modified to determine design values for the limiting force for the deformable connection at each floor of the building. The modified calculations are shown in the following equations:

$$F_{Lx} = \frac{C_{Lx}}{R_{DC}} \frac{w_{px}}{n_{Lx}} \tag{7}$$

$$C_{L0} = 0.4 S_{DS} I_e \tag{8}$$

$$C_{Ln} = \sqrt{(\Gamma_{m1} C_s)^2 + (\Gamma_{m2} C_{s2})^2} \tag{9}$$

where F_{Lx} is the design limiting force for the deformable connection at level x, which is the target force value when the connection response transitions from linear-elastic to post-elastic, C_{Lx} is the design acceleration coefficient at level x, C_{Ln} is the design acceleration coefficient at level n, C_{L0} is design acceleration coefficient at the base of the building, and R_{DC} is the deformable connection design force factor that accounts for the deformation capacity of the deformable connection. Specific values are not given for R_{DC} in this section. Possible values of R_{DC} will be assessed and discussed later. w_{px} is the seismic weight tributary to the diaphragm at level x, n_{Lx} is the number of force-limiting deformable connections at level x, S_{DS} is the design spectral acceleration at short periods, and I_e is the importance factor (FEMA 2015). C_{Lx} and F_{Lx} for $n \geq 3$ (assuming w_{px}, R_{DC}, and n_{LX} are the same for each floor) are shown in Fig. 4. F_{Lx} is used to design the force-limiting deformable connections at level x.

The calculations were modified to seek a balanced distribution of inelastic deformation demand between the force-limiting deformable connections and the flexural yielding base mechanism of the LFRS. The modifications are the following: (1) The participation of the first mode in C_{Ln} in Equation 9 is not amplified by the LFRS overstrength factor Ω_0 in comparison to C_{pn} in Equation 3 since the calculation of F_{Lx} assumes that no significant hardening has occurred at the base flexural yielding mechanism of the LFRS when the force-deformation responses of the deformable connections transition from linear-elastic to post-elastic. (2) The lower limit is not used for F_{Lx} in

Equation 7 in comparison to F_{px} from Equation 1. (3) The factor R_{DC} accounts for the deformation capacity (i.e., ductility capacity) of the deformable connections instead of the diaphragm design force reduction factor R_s used in Equation 1. The base moment in the LFRS, M_{bFLx}, calculated assuming the F_{Lx} act concurrently, should be greater than or equal to M_{by}, which is the moment when nonlinear moment-rotation response initiates at the base flexural yielding mechanism of the LFRS. $M_{bFLx}/M_{by} \geq 1.0$ is intended to prevent excessive deformation demands in the force-limiting connections and balance the inelastic deformations between the LFRS and connections. An upper limit on R_{DC} is developed as follows:

$$
\begin{aligned}
1.0 &\leq \frac{M_{bFLx}}{M_{by}} \\
1.0 &\leq \sum_{x=1}^{n} \frac{F_{Lx} h_x}{M_{by}} \\
1.0 &\leq \sum_{x=1}^{n} \frac{\frac{C_{Lx}}{R_{DC}} \frac{w_{px}}{n_{Lx}} h_x}{M_{by}} \\
R_{DC} &\leq \sum_{x=1}^{n} \frac{C_{Lx} \frac{w_{px}}{n_{Lx}} h_x}{M_{by}}
\end{aligned} \tag{10}
$$

The proposed method enables the preliminary design of the force-limiting deformable connections without a large number of parametric numerical earthquake simulations. Nonlinear numerical earthquake simulations are needed to determine if the building seismic response is acceptable.

Design of force-limiting deformable connections for example buildings

This section presents designs for force-limiting deformable connections for twelve-story, eight-story, and four-story reinforced concrete shear wall building models from the method proposed in the previous section. Various R_{DC} values are considered. Later in the paper, the seismic responses from numerical simulations of twelve-story, eight-story, and four-story buildings with connections designed using the various R_{DC} values are compared with the seismic responses of twelve-story, eight-story, and four-story buildings with deformable connections with a constant limiting force F_L over the height of the building, and with the seismic responses of twelve-story, eight-story, and four-story buildings with RE connections, which represent conventional buildings.

Reinforced concrete shear wall example buildings

The example buildings are bearing wall systems with special reinforced concrete shear walls (ASCE 2017). Fig. 5(a) shows the typical floor plan for the twelve-story, eight-story, and four-story buildings. The floor plan dimensions are 30.5 m x 55.0 m. The ASCE/SEI 7 design spectrum parameters that were used are $S_1 = 0.6g$, $S_s = 1.5g$, $F_a = 1.0$, $F_v = 1.5$, $T_{long} = 8.0$ seconds, Site Class D, and Importance Factor $I_e = 1.0$ (ASCE 2017). The first story height is 4.9 m and the remaining story heights are 3.2 m for all three buildings. Symmetry along both plan directions enabled one half of the building to be modeled and studied. The area tributary to the shear wall and the gravity system in the model is shown in Fig. 5(a). Each shear wall was assumed to resist half of the seismic-induced horizontal forces along its plane. The equivalent horizontal seismic force method was used to design the shear wall of each building (ASCE 2017). The moment at the base of the shear wall due to the equivalent horizontal seismic forces is denoted M_{ELF1}.

Design values for limiting force for deformable connection at each floor of the example buildings

The parameters required to calculate C_{Lx} for the twelve-story building are parameters for the design spectrum: I_e = 1.0, S_{DS} = 1.0, and S_{D1} = 0.6, and parameters for the building: z_s = 1.0, n = 12, C_s = 0.1104, C_{s2} = 1.0, Γ_{m1} = 1.4583, Γ_{m2} = 0.7563, C_{L0} = 0.4, and C_{Ln} = 0.7732. Table 1 lists the quantities required for the calculation of F_{Lx} used in the deformable connections in the twelve-story building with R_{DC} = 3.0. The parameters for the eight-story building are: z_s = 1.0, n = 8, C_s = 0.1473, C_{s2} = 1.0, Γ_{m1} = 1.4375, Γ_{m2} = 0.6891, C_{L0} = 0.4, and C_{Ln} = 0.7209; and the parameters for the four-story building are: z_s = 1.0, n = 4, C_s = 0.2, C_{s2} = 0.85, Γ_{m1} = 1.3750, Γ_{m2} = 0.5063, C_{L0} = 0.4, and C_{Ln} = 0.5107. Fig. 6 shows profiles of F_{Lx} over the height of the building (i.e., design limiting force values) and the two cases of constant F_L over the height of the building (denoted as F_{L1-1} and F_{L1-2}), for the twelve-story, eight-story, and four-story buildings. For reference, Fig. 6 also includes the one half of the F_{px} force profile based on ASCE7-10 (ASCE 2010) and the one half of the F_{px} force profile based on Eq. (1). The values of R_{DC} used in the design examples satisfy the inequality condition in Eq. (10). For example, for the twelve-story building a value of $R_{DC} = 3.0$ results to $M_{bFLx}/M_{by} = 1.04 > 1.0$. Larger values of R_{DC} would result to $M_{bFLx}/M_{by} < 1.0$.

COMPARISON OF SEISMIC RESPONSES OF BUILDINGS FROM NUMERICAL SIMULATIONS

Reinforced concrete shear wall example building numerical models

Fig. 5(b) shows a schematic of the typical numerical model used for the twelve-story, eight-story, and four-story buildings. Linear-elastic beam-column elements were used to model the stiffness of the LFRS (shear wall) and GLRS. Nonlinear flexural response and shear failure were not included in these elements. For the numerical simulations used to determine the seismic response, nonlinear flexural response at the base of the wall, shown in Fig. 5(d), was modeled with a nonlinear spring at the base of the wall (described below). Geometric nonlinearities were considered. Table 2 lists properties of the linear-elastic beam-column elements used to model the shear wall and properties of the base hinge spring used to model the base moment-rotation nonlinear response of the shear wall. The wall area A_w, the wall cracked moment of inertia about the strong axis I_{crw}, and the concrete modulus of elasticity E_c, are given for the beam-column elements used to model the shear wall in each building model.

The yield strength and the ultimate capacity of the base hinge spring element, M_{by}, and M_{bcap}, respectively, are given in Table 2. The OpenSees (McKenna and Fenves 2021) uniaxial material model Pinching4 was used to model the LFRS base hinge nonlinear moment-rotation response shown in Fig. 5(d) along with the parameters $rDispP$, $rForceP$, $uForceP$, $gK1$, $gK2$, $gK3$, $gK4$, $gKLim$, $gD1$, $gD2$, $gD3$, $gD4$, $gDLim$, $gF1$, $gF2$, $gF3$, $gF4$, $gFLim$, gE, and $dmgType$ that are equal to 0.85, 0.85, 0.05, 1.0, 0.0, 0.0, 0.0, 0.995, 0.0, 0.0, 0.0, 0.0, 0.0, 0.0, 0.0, 0.0, 0.0, 0.0, 10, and "cycle", respectively. A pin-base lean-on column is used to model the GLRS in all buildings, which results in an upper bound of the connection deformation demand (Tsampras

2016). Table 3 lists the modulus of elasticity E_c, the area A_c, and the moment of inertia I_c of the linear-elastic beam-column elements used for the lean-on column in each building model. The section properties A_c and I_c listed in Table 3 are estimated considering the sum of the properties of the gravity columns within the area tributary to the shear wall. I_c is estimated considering the cracked moment of inertia of each gravity column.

Fig. 5(c) shows the typical force-limiting deformable connection force-deformation response. The deformable connections are designed as friction devices and low damping rubber bearings (Tsampras et al. 2018). All the deformable connections have elastic stiffness K_{el} = 1730 kN/mm and post-elastic stiffness ratio a = 0.005. F_L (Fig. 5(c)) were discussed in previous section and presented in Fig. 6. The buildings with RE connections have connections that are essentially rigid and remain linear-elastic, with stiffness equal to 4340 MN/mm.

Numerical simulations results

In this section, results from numerical earthquake simulations of the twelve-story, eight-story, and four-story buildings with force-limiting deformable connections with F_{Lx} designed with various R_{DC} values are compared with the results from numerical earthquake simulations of the twelve-story, eight-story, and four-story buildings with force-limiting deformable connections with constant F_L over the height of the building or with RE connections.

Eighteen ground motions listed in Table 4 were selected from the FEMA P-695 (FEMA 2009) far field set and used as input excitation in the numerical earthquake simulations. Each recorded ground motion was scaled so that the average response spectrum of the scaled ground motions (Baker 2011) matches the spectral accelerations to the ASCE/SEI 7 (ASCE 2017) design basis earthquake spectrum over a range of periods T∈[0.6, 2.0] seconds, as shown in Figure 7. All the numerical simulations were performed using design basis earthquake level ground motions.

Fig. 8 shows seismic responses from numerical simulations for twelve-story buildings. Fig. 9 shows seismic responses from numerical simulations for eight-story and four-story buildings. The responses plotted in these figures are the floor total acceleration, the force and the deformation in the connections between the floor-diaphragm of the GLRS and the LFRS, the story shear and the drift of the LFRS, and the story shear and the drift of the GLRS. The peak value of the response that occurs during each ground motion at each floor or story is shown with a colored marker. The different colors represent the different cases of the force-limiting deformable connections between the floors and the LFRS designed with different values for the limiting force; either F_{Lx} for different R_{DC} values, or a constant F_L over the height of the building. The mean value of the peak responses at each floor or story over the set of ground motions is shown with a white marker for each connection case. The statistics of the maximum peak floor or story responses of the twelve-story building shown in Fig. 8 are listed in Table 5, where the "maximum" is the maximum over the floors or stories of the building, and the statistics are over the ground motions in the set. μ, σ, and σ/μ denote the mean value, the standard deviation, and the coefficient of variation, respectively. A discussion on the observations related to each response quantity is presented in the following paragraphs.

Floor total accelerations

The mean peak values of the floor total accelerations and their dispersion is significantly reduced for the twelve-story buildings with various deformable connection designs compared to those of the twelve-story building with RE connections. The coefficient of variation of the maximum peak floor total acceleration in the buildings with force-limiting deformable connections is approximately half the coefficient of variation of the maximum peak floor total acceleration in the building with RE connections.

The mean peak values of the floor total accelerations and their dispersion for the eight-story and four-story buildings with deformable connections are smaller than those of the eight-story and four-story buildings with RE connections. The eight-story and four-story buildings with deformable connections have similar floor total accelerations.

As will be shown later, these observations are attributed to the ability of the force-limiting deformable connections to mitigate the contribution of the second mode to the total seismic response.

Force-limiting deformable connection forces

The mean peak values of the connection forces and their dispersion for the twelve-story buildings with various force-limiting deformable connection designs are significantly reduced compared to those of the twelve-story building with RE connections. The connection forces for the twelve-story buildings with deformable connections are similar, however, the twelve-story building with deformable connections with F_{Lx} based on $R_{DC} = 3.0$ has the smallest connection forces. The coefficient of variation for the maximum peak connection force in the buildings with deformable connections is approximately one fifth of the coefficient of variation for the maximum peak connection force in the building with RE connections.

The eight-story and four-story buildings with deformable connections have connection forces that are less than those of the eight-story and four-story buildings with RE connections. The connection forces at the sixth floor of the eight-story buildings with deformable connections are close to the connection force at the sixth floor of the eight-story building with RE connections. The sixth floor of the eight-story building is at 0.77 of the total height of the building which is close to the node of the second mode shape. A similar observation can be made for the third-floor of the four-story building and the tenth-floor of the twelve-story building.

LFRS (shear wall) story shears

The use of force-limiting deformable connections in the twelve-story buildings reduces the mean peak LFRS story shears and their dispersion compared to the LFRS story shears of the twelve-story building with RE connections. The LFRS story shears in the twelve-story buildings with various deformable connection designs are similar, however, the connections with F_{Lx} based on $R_{DC} = 3.0$ result in the smallest mean peak LFRS base (i.e., first story) shear. Note that the mean peak LFRS base shears exceed significantly the design base shear calculated using the ASCE/SEI 7 equivalent lateral force procedure (7835 kN). However, the use of deformable connections reduces the ratio of the mean peak LFRS first story shear over the design base shear. The coefficient of variation for the maximum peak LFRS story shear in the buildings with deformable connections is approximately one quarter of the coefficient of variation for the maximum peak LFRS story shears in the building with RE connections.

The eight-story and four-story buildings with various deformable connection designs also have reduced mean peak LFRS story shears and reduced dispersion of the peak LFRS story shears compared to those of the eight-story and four-story buildings with RE connections. The eight-story buildings with deformable connections have similar LFRS story shears, and the four-story buildings with deformable connections have similar LFRS story shears.

Gravity load resisting system (GLRS) story shears

The twelve-story building with RE connections has GLRS story shears in the second and upper stories with magnitude and dispersion that are less than those of the buildings with force-limiting deformable connections. As expected, the story shears in the GLRS are significantly less than those in the LFRS.

The eight-story and four-story buildings with various deformable connection designs have similar GLRS story shears over the height of the building. The magnitude and dispersion of GLRS story shears in the upper stories are larger than those of the eight-story and four-story buildings with RE connections. The twelve-story buildings with deformable connections also have GLRS story shears with magnitude similar to those of the eight-story and four-story buildings with deformable connections.

Force-limiting deformable connection deformations

The twelve-story buildings with force-limiting deformable connections designed for F_{Lx} that varies over the height of the building have a more uniform connection deformations over the height of the building compared to the twelve-story buildings with deformable connections designed for F_{L1-1} and F_{L1-2} that do not vary over the height of the building. For F_{Lx} with a small R_{DC} value, $R_{DC} \leq 1.5$, the connection deformations are nearly constant over the height of the building, and for a large R_{DC} value, $R_{DC} = 3.0$, the connection deformations increase over the height of the building. At the twelfth-floor, where the connection deformation is largest, the connection deformation was smaller with F_{Lx} based on $R_{DC} = 3.0$ than for constant F_{L1-1}, even though F_{Lx} based $R_{DC} = 3.0$ does not exceed F_{L1-1} (for floors 1 through 9, F_{Lx} with $R_{DC} = 3.0$ is $0.50F_{L1-1}$, and for floors 10, 11, and 12, F_{Lx} with $R_{DC} = 3.0$ is $0.59F_{L1-1}$, $0.78F_{L1-1}$, and $0.97F_{L1-1}$, respectively).

The eight-story buildings with deformable connections designed for F_{Lx} have smaller connection deformations at the top two floors compared to the eight-story buildings with deformable connections designed for F_{L1-1} and F_{L1-2}. The four-story buildings with deformable connections designed for F_{Lx} based on $R_{DC} = 1.5$ or 1.7 have connection deformations similar to those of the four-story buildings with deformable connections designed for F_{L1-1} and F_{L1-2}. The four-story buildings with deformable connections designed for F_{Lx} based on $R_{DC} \leq 1.2$ have connection deformations at the top two floors that are smaller than the connection deformations at the top two floors of the four-story buildings with deformable connections designed for F_{L1-1} and F_{L1-2}.

LFRS (shear wall) story drifts

The LFRS story drifts in all buildings are relatively uniform over the height of the building. The twelve-story buildings with force-limiting deformable connections have smaller LFRS story drifts than the building with RE connections. The twelve-story building with deformable connections designed for F_{Lx} with $R_{DC} = 3.0$ has the smallest LFRS story drifts.

The eight-story and four-story buildings with deformable connections also have smaller LFRS drifts than the eight-story and four-story buildings with RE connections, respectively.

Gravity load resisting system (GLRS) story drifts

The twelve-story buildings with force-limiting deformable connections designed for F_{L1-1} and F_{L1-2} have larger GLRS drifts in the top two stories compared to the building with RE connections. The twelve-story buildings with deformable connections designed for F_{Lx} have smaller or similar GLRS story drifts compared to those of the twelve-story building with RE connections.

The GLRS story drifts in the top two stories of the eight-story buildings with deformable connections designed for F_{L1-1} and F_{L1-2} are larger than the GLRS story drift in the top two stories of the eight-story building with RE connections. The eight-story buildings with deformable connections designed for F_{Lx} have GLRS story drifts smaller than or similar to the GLRS story drifts of the eight-story building with RE connections. The four-story buildings with deformable connections have larger GLRS story drifts in the top story compared to the four-story building with

RE connections. However, the four-story buildings with deformable connections have GLRS drifts in the remaining stories similar to those of the four-story building with RE connections.

Effect of R_{DC} and number of stories

This section presents a discussion on the effect of the R_{DC} value and the number of building stories on the mean of the maximum peak floor or story seismic responses. Each individual plot in Fig. 10 shows the mean of the maximum peak value of a seismic response on the y-axis with respect to the R_{DC} values on the x-axis. The twelve-story, eight-story, and four-story building results are shown with black circles, red rectangles, and white triangles, respectively. Row 1 of the plots in Fig. 10 shows the mean maximum peak value of seismic responses of buildings with force-limiting deformable connections designed for F_{Lx} with various R_{DC} values, denoted μ_{FLx}. Row 2 of the plots in Fig. 10 show μ_{FLx} normalized by the mean maximum peak value of the seismic response of buildings with force-limiting deformable connections with F_{L1-1}, denoted μ_{FL1-1}. Row 3 of the plots in Fig. 10 shows μ_{FLx} normalized by the seismic responses of buildings with RE connections, denoted μ_{RE}.

The values of μ_{FLx} for the connection deformation depend on the number of stories and the R_{DC} value. The connection deformation $\mu_{FLx} \approx 50$ mm and $\mu_{FLx}/\mu_{FL1-1} \approx 0.5$ in twelve-story, eight-story, and four-story buildings when R_{DC} equals 2, 1.5, and 0.8, respectively. The connection deformation $\mu_{FLx}/\mu_{FL1-1} < 1.0$ for every R_{DC} values and number of stories, while it approaches 1.0 when $R_{DC} = 1.7$ or 1.5 in the four-story building. Thus, four-story buildings require smaller R_{DC} values than eight-story and twelve-story buildings to ensure reasonable connection deformations μ_{FLx}. The deformation in the RE connections is essentially zero. Thus, μ_{FLx}/μ_{RE} is not defined for the connection deformation response and no plot is not shown in the first column of the third row in Fig. 10.

The floor acceleration and connection force μ_{FLx} depend on R_{DC} but they are essentially independent of the number of stories. The floor acceleration and connection force $\mu_{FLx}/\mu_{FL1-1} \leq 1.0$ for $R_{DC} \geq 1.5$, and $\mu_{FLx}/\mu_{RE} \leq 0.75$ for every R_{DC} value.

The LFRS story shear μ_{FLx} depends on R_{DC} and the number of stories. The LFRS story shear μ_{FLx} decreases as the number of stories decreases. The LFRS story shear μ_{FLx} decreases as R_{DC} increases. The LFRS story shear results μ_{FLx}/μ_{FL1-1} and μ_{FLx}/μ_{RE} are essentially independent of the number of stories. The LFRS story shear $\mu_{FLx}/\mu_{FL1-1} \leq 1.0$ for $R_{DC} \geq 1.5$, and $\mu_{FLx}/\mu_{RE} \leq 0.8$ for every R_{DC} value.

The GLRS story shear μ_{FLx} depends on the number of stories but it is not affected significantly by R_{DC}. The GLRS story shear results μ_{FLx}/μ_{FL1-1} and μ_{FLx}/μ_{RE} are similar and approximately equal to 1.0 for all R_{DC} and number of stories, with exception the four-story building which has GLRS story shear $\mu_{FLx}/\mu_{RE} > 1.5$ for all R_{DC}.

The LFRS story drift μ_{FLx} depends on R_{DC} and the number of stories. As R_{DC} increases the LFRS story drift μ_{FLx} decrease. The effect of R_{DC} on the change of LFRS story drift μ_{FLx} is more significant for the four-story building compared to the eight-story and twelve-story buildings. However, the LFRS story drift μ_{FLx} remain less than 1.2% for all R_{DC} and number of stories. The LFRS story drift $\mu_{FLx}/\mu_{FL1-1} \leq 1.0$ for $R_{DC} \geq 1.7$ for all number of stories while it approaches a maximum value of 2.0 in the four-story building with $R_{DC} = 0.8$. All buildings have LFRS story drift $\mu_{FLx}/\mu_{RE} \leq 1.0$.

The GLRS story drift μ_{FLx} in the eight-story and twelve-story buildings is similar and essentially independent of R_{DC}. The GLRS story drift μ_{FLx} in the four-story building increases as R_{DC} decreases and it is approximately equal to 2% for $R_{DC} = 0.8$. All buildings have $\mu_{FLx}/\mu_{FL1-1} \leq 1.0$. The twelve-story and eight-story buildings have GLRS story drift $\mu_{FLx}/\mu_{RE} \approx 1.0$. However, for the four-story buildings, as R_{DC} decreases the GLRS story drift μ_{FLx}/μ_{RE} increases.

Variation of the twelve-story building periods of vibration under strong ground motion

This section shows the effect of force-limiting deformable connections on the second mode seismic response of the twelve-story building. More specifically, this section compares the time variation of the periods of vibration of the building with RE connections with the time variation of the periods of vibration of the building with deformable connections designed for F_{Lx} with R_{DC} = 3.0, 2.0, and 0.8, during the first ten seconds of the ground motion EQ1 (listed in Table 4).

In general, the periods of vibration of a linear-elastic building model are determined from its mass matrix and stiffness matrix. The nonlinear response of a building model changes the tangent stiffness during the response history while the mass remains constant. In this study, the first and second mode periods of vibration of the building models are calculated at the end of each converged time step of the nonlinear time history analysis from the constant mass matrix and tangent stiffness matrix.

Fig. 11(a) shows the first ten seconds of EQ1 ground acceleration time history. At approximately 3.5 seconds, strong ground acceleration initiates and at approximately 7.0 seconds it ends. Fig. 11(b) shows the pseudo-acceleration response spectrum of EQ1 in comparison with the ASCE/SEI 7 design response spectrum. EQ1 has significantly larger spectral acceleration in the period region between 0.1 seconds and 0.5 seconds.

Fig. 11(c) through (e) show the time variation of the first mode period of vibration for the twelve-story building with RE connections and the time variation of the first mode period of vibration for building models with force-limiting deformable connections designed for F_{Lx} with R_{DC} = 3.0, 2.0, and 0.8, respectively, during the first ten seconds of EQ1. After the initiation of strong ground acceleration, the first mode periods of the buildings increase. As R_{DC} decreases the time variation of the first mode period in the buildings with force-limiting deformable connections approaches the variation of the first mode period in the building with RE connections. Deformable connections with smaller R_{DC} values have larger connection forces. The larger connection forces are transferred to the LFRS and develop larger LFRS story drift demand. The larger LFRS story drift demand results to leads to larger nonlinear rotation responses and reduced stiffness at the base flexural hinge of the LFRS (shear wall). As a result, the first mode period of vibration at the end of the strong ground motion acceleration approaches the first mode period of vibration of the building with RE connections.

Fig. 11(f) through (h) show the time that the second mode period of the building with RE connections is approximately constant while the second mode periods of the buildings with deformable connections are increased during the time of strong ground acceleration. As R_{DC} decreases the variation of the second mode period is decreased.

Fig. 11(i) through (k) show the twelfth-floor total acceleration in the twelve-story building model with RE connections and twelfth-floor total acceleration in the building models with deformable connections. The deformable connections reduce the twelfth-floor total accelerations during and after the time of strong ground acceleration. At approximately 5.5 seconds of the time history, the twelfth-floor total acceleration of the building model with RE connections has large-amplitude response with an approximate period of 0.3 seconds which is close to the second mode period observed in Fig. 11(f) through (h); this result shows the importance of the second mode response to these large floor total accelerations. It is also noted that the twelve-story building model with deformable connections with smaller R_{DC} values have larger floor total accelerations during the time of the strong ground acceleration. Fig. 11(i) through (n) show the tenth-floor total acceleration in the building model with RE connections and the tenth-floor total acceleration in the building models with deformable connections. The tenth-floor is close to the node of the second mode shape of the building, and therefore, the tenth-floor total acceleration amplitude is significantly smaller than the twelfth-floor total acceleration amplitude in the building with RE connections. The tenth-floor total acceleration amplitude is similar to the twelfth-floor total acceleration amplitude in the building models with deformable connections.

These observations show that the force-limiting deformable connections modify the second mode seismic response of the twelve-story building while the nonlinear moment-rotation flexural base hinge response of the LFRS (shear wall) modifies primarily the first mode seismic response of the twelve-story building. The observations show that the effect of deformable connections on the seismic response of the building mitigates the contribution of the second mode to the total seismic response.

Summary

This paper presented (1) a force-based design method to determine the design value of the limiting force for the force-limiting deformable connection at each floor of buildings with LFRS that have a base flexural mechanism (e.g., reinforced concrete shear wall buildings), (2) design examples, and (3) numerical simulations of twelve-story, eight-story, and four-story reinforced concrete shear wall example buildings with force-limiting deformable connections designed using the proposed method. The proposed design method is a modified version of the ASCE/SEI 7-16 (ASCE 2017) alternative seismic design force method for floor-diaphragms. The method is simple to implement in design practice. The method is also efficient since it does not require large number of parametric numerical earthquake simulations to determine feasible design space for the design values of the limiting force. The method provides design values for the limiting force that vary appropriately over the height of the building by considering the relative contributions of the first and higher modes to the seismic response of a building. The design examples showed the design values for the limiting forces of force-limiting deformable connections for twelve-story, eight-story, and four-story reinforced concrete shear wall example buildings. Seismic responses from numerical simulations of these example buildings with force-limiting deformable connections designed using the proposed design method were compared with the seismic responses of the example buildings with deformable connections with a constant limiting force over the height of the building, and with the seismic responses of the example buildings with RE connections, which represent conventional buildings. The effect of number of stories in the building and the magnitude of the limiting forces on the seismic response of the example buildings was studied. It was shown that the buildings with force-limiting deformable connections designed using the proposed method have a more uniform distribution of connection deformation demands over the height of the building compared to the buildings with deformable connections with a constant limiting force values over the height of the building. Larger design values of limiting force are required in the four-story building to have connection deformation demands similar to those of the eight-story and the twelve-story buildings. It was also shown that the buildings with force-limiting deformable connections designed using the proposed method have floor accelerations and force responses with reduced magnitude and dispersion compared to buildings with RE connections.

Conclusions

- The proposed force-based method for design of force-limiting deformable connections enables simple and efficient calculation of the limiting force values required for preliminary design of these deformable connections that control the transfer of seismic-induced horizontal forces from the floor-diaphragms to the LFRS.
- Buildings with force-limiting deformable connections designed using the proposed method have reasonable connection deformation demands and relatively uniform distribution connection deformation demands over the height of the building.
- As the number of stories of the building decreases, F_{Lx} based on smaller R_{DC} value is required for reasonable connection deformation demands. It was observed that values of R_{DC} close to 1.5 for the twelve-story and the eight-story buildings and 1.0 for the four-story building result in acceptable seismic responses, even when a pin-based lean-on column model is assumed for the gravity load resisting system.
- The use of force-limiting deformable connections designed using the proposed method mitigates the contributions of the second mode response to the total seismic response of a building.

The proposed method is aimed at the preliminary design of force-limiting connections. Numerical simulations of the building with force-limiting deformable connections may be needed to assess the seismic response of the force-limiting connections, the LFRS, and the GLRS.

Data Availability Statement

Some or all data, models, or code that support the findings of this study are available from the corresponding author upon reasonable request. Experimental data from previous research conducted for the development of the force-limiting deformable connections and the development of the friction devices referenced in this paper are available at DesignSafe-CI (Tsampras and Sause

2014a; Tsampras and Sause 2014b; Fleischman et al. 2014).

Acknowledgments

The authors are grateful for financial support provided by the Lehigh University and the Advanced Technology for Large Structural Systems (ATLSS) Engineering Research Center. Any opinions, findings, and conclusions expressed in this paper are those of the authors and do not necessarily reflect the views of others acknowledged here.

REFERENCES

ASCE, ed. (2010). *Minimum Design Loads for Buildings and Other Structures*. ASCE Standard. American Society of Civil Engineers : Structural Engineering Institute, Reston, Va.

ASCE (2017). *Minimum Design Loads*. ASCE, Reston, VA, seventh edition, https://doi.org/10.1061/9780784414248.

Baker, J. W. (2011). "Conditional Mean Spectrum: Tool for Ground-Motion Selection." *Journal of Structural Engineering*, 137(3), 322–331, https://doi.org/10.1061/(ASCE)ST.1943-541X.0000215.

Cao, L., Marullo, T., Al-Subaihawi, S., Kolay, C., Amer, A., Ricles, J., Sause, R., and Kusko, C. S. (2020). "NHERI Lehigh Experimental Facility With Large-Scale Multi-Directional Hybrid Simulation Testing Capabilities." *Frontiers in Built Environment*, 6, 107, https://doi.org/10.3389/fbuil.2020.00107.

Crane, S. T. (2004). "Influence of energy dissipation connections between floors and the lateral force resisting system." *Report no.*, MS Thesis, UC San Diego, USA.

FEMA (2009). "Quantification of Building Seismic Performance Factors." *Report No. FEMA P-695*, Federal Emergency Management Agency.

FEMA (2015). "NEHRP Recommended Seismic Provisions for New Buildings and Other Structures." *Report No. P-1050-1/2015*, Federal Emergency Management Agency.

FEMA (2017). "Guidelines for nonlinear structural analysis and design of buildings. part I - general." *Report No. NIST GCR 17-917-46v1*, National Institute of Standards and Technology, Gaithersburg, MD, https://doi.org/10.6028/NIST.GCR.17-917-46v1.

Fleischman, R., Restrepo, J., Nema, A., Zhang, D., Shakya, U., Zhang, Z., Sause, R., Tsampras, G., and Monti, G. (2015). "Inertial Force-Limiting Anchorage System for Seismic Resistant Building Structures." *Structures Congress*, Portland, Oregon, Structures Congress, 1302–1313, https://doi.org/10.1061/9780784479117.111.

Fleischman, R. B. and Farrow, K. T. (2001). "Dynamic behavior of perimeter lateral-system structures with flexible diaphragms." *Earthquake Engineering & Structural Dynamics*, 30(5), 745–763, https://doi.org/10.1002/eqe.36.

Fleischman, R. B., Restrepo, J. I., Sause, R., Zhang, D., Tsampras, G., Zhang, Z., Nema, A., and Shakya, U. (2014). "Half Scale Shake Table Test of a 4 Story Reinforced Concrete Building with Eccentric Shear Walls, https://doi.org/10.4231/D39W0908G.

McKenna, F. and Fenves, G. (2021). "The OpenSees Command Language Manual.

Moehle, J. P., Hooper, J. D., Kelly, D. J., and Meyer, T. R. (2010). "Seismic Design of Cast-in-Place Concrete Diaphragms, Chords, and Collectors." *Report No. NIST GCR 10-917-4*, National Institute of Standards and Technology.

Ray-Chaudhuri, S. and Hutchinson, T. C. (2011). "Effect of Nonlinearity of Frame Buildings on Peak Horizontal Floor Acceleration." *Journal of Earthquake Engineering*, 15(1), 124–142, https://doi.org/10.1080/13632461003668046.

Rodriguez, M. E., Restrepo, J. I., and Carr, A. J. (2002). "Earthquake-induced floor horizontal accelerations in buildings." *Earthquake Engineering & Structural Dynamics*, 31(3), 693–718, https://doi.org/10.1002/eqe.149.

Sattar, S., McAllister, T., Johnson, K., Clavin, C., Segura, C., McCabe, S., Fung, J., Abrahams, L., Sylak-Glassman, E., Levitan, M., Harrison, K., and Harris, J. (2018). "Research needs to support immediate occupancy building performance objective following natural hazard events." *Report No. NIST SP 1224*, National Institute of Standards and Technology, Gaithersburg, MD, https://doi.org/10.6028/NIST.SP.1224.

Tsampras, G. (2016). “Force-Limiting Floor Diaphragm Connection for Earthquake-Resistant Buildings.” Ph.D. thesis, Lehigh University, USA, https://preserve.lib.lehigh.edu/islandora/object/preserve%3Abp-10369972.

Tsampras, G. and Sause, R. (2014a). “Full-scale, components test of Inertial Force-Limiting Floor Anchorage Systems for Seismic Resistant Building Structures using a Buckling Restrained Brace and Steel Reinforced Low Damping Rubber Bearings, https://doi.org/10.4231/D3N87311M.

Tsampras, G. and Sause, R. (2014b). “Full-scale, components test of Inertial Force-Limiting Floor Anchorage Systems for Seismic Resistant Building Structures using a Friction Device and Carbon Fiber Reinforced Low Damping Rubber Bearings, https://doi.org/10.4231/D3HH6C68B.

Tsampras, G., Sause, R., Fleischman, R. B., and Restrepo, J. I. (2017). “Experimental study of deformable connection consisting of buckling-restrained brace and rubber bearings to connect floor system to lateral force resisting system.” *Earthquake Engineering & Structural Dynamics*, 46(8), 1287–1305, https://doi.org/10.1002/eqe.2856.

Tsampras, G., Sause, R., Fleischman, R. B., and Restrepo, J. I. (2018). “Experimental study of deformable connection consisting of friction device and rubber bearings to connect floor system to lateral force resisting system.” *Earthquake Engineering & Structural Dynamics*, 47(4), 1032–1053, https://doi.org/10.1002/eqe.3004.

Tsampras, G., Sause, R., Zhang, D., Fleischman, R. B., Restrepo, J. I., Mar, D., and Maffei, J. (2016). “Development of deformable connection for earthquake-resistant buildings to reduce floor accelerations and force responses.” *Earthquake Engineering & Structural Dynamics*, 45(9), 1473–1494, https://doi.org/10.1002/eqe.2718.

Van Den Einde, L., Conte, J. P., Restrepo, J. I., Bustamante, R., Halvorson, M., Hutchinson, T. C., Lai, C.-T., Lotfizadeh, K., Luco, J. E., Morrison, M. L., Mosqueda, G., Nemeth, M., Ozcelik, O., Restrepo, S., Rodriguez, A., Shing, P. B., Thoen, B., and Tsampras, G. (2021). “NHERI@UC San Diego 6-DOF Large High-Performance Outdoor Shake Table Facility.” *Frontiers in Built Environment*, 6, 181, https://doi.org/10.3389/fbuil.2020.580333.

Zhang, D., Fleischman, R., Restrepo, J., Sause, R., Maffei, J., Mar, D., and Monti, G. (2014). "Development of a Floor Inertial Force Limiting Anchorage System Building Seismic Response." *10th U.S. National Conference on Earthquake Engineering*, 10th U.S. National Conference on Earthquake Engineering, 11.

Zhang, Z., Fleischman, R. B., Restrepo, J. I., Guerrini, G., Nema, A., Zhang, D., Shakya, U., Tsampras, G., and Sause, R. (2018). "Shake-table test performance of an inertial force-limiting floor anchorage system." *Earthquake Engineering & Structural Dynamics*, 47(10), 1987–2011, https://doi.org/10.1002/eqe.3047.

List of Tables

1 Twelve-story building F_{Lx} for R_{DC} = 3.0. 29
2 Properties of the shear wall element. 30
3 Properties of the gravity column elements. 31
4 Eighteen ground motions selected from 44 FEMA P-695 far-field earthquake ground motion set. 32
5 Statistics of seismic responses for twelve-story buildings. 33

TABLE 1. Twelve-story building F_{Lx} for R_{DC} = 3.0.

Level x	h_x/h_n	n_{Lx}	w_{px}/n_{Lx}	C_{Lx}	F_{Lx}	$M_{F_{Lx}}$	$M_{bF_{Lx}}/M_{by}^{a}$
[−]	[−]	[−]	[kN]	[−]	[kN]	[MNm]	[−]
12	1.00	2	5916	0.77	1525	5	-
11	0.92	2	5916	0.62	1231	14	-
10	0.84	2	5916	0.48	937	26	-
9	0.76	2	5916	0.40	789	40	-
8	0.68	2	5916	0.40	789	57	-
7	0.60	2	5916	0.40	789	76	-
6	0.52	2	5916	0.40	789	98	-
5	0.44	2	5916	0.40	789	122	-
4	0.36	2	5916	0.40	789	149	-
3	0.28	2	5916	0.40	789	179	-
2	0.20	2	5916	0.40	789	211	-
1	0.12	2	5916	0.40	789	264	1.04

[a] M_{by} = 253 MNm

TABLE 2. Properties of the shear wall element.

	Beam-Column Elements			Base Hinge Spring Element	
Building	A_w	I_{wcr}	E_c	$M_{by} = \frac{M_{ELF1}}{\phi^a}$	M_{bcap}
[−]	[m^2]	[m^4]	[MPa]	[MNm]	[MNm]
12-Story	6.50	31.10	27800	253.0	569.0
8-Story	5.40	18.00	27800	154.0	384.0
4-Story	3.10	3.40	27800	58.0	145.0

[a] $\phi = 0.9$

TABLE 3. Properties of the gravity column elements.

Building [−]	Stories [−]	E_c [MPa]	A_c [m^2]	I_c [m^4]
12-Story	1^{st}-6^{th}	27800	10.5700	0.4070
12-Story	7^{th}-12^{th}	27800	4.9960	0.0910
8-Story	1^{st}-4^{th}	27800	6.9780	0.2540
8-Story	5^{th}-8^{th}	27800	3.7260	0.0720
4-Story	1^{st}-4^{th}	27800	3.7260	0.0720

TABLE 4. Eighteen ground motions selected from 44 FEMA P-695 far-field earthquake ground motion set.

EQ [#]	Event [−]	Moment Magnitude [−]	Year [−]	Distance [km]	Soil Type Class [−]	Component [−]	PGA[a] [g]	PGV[a] [cm/sec]	SF[b] [−]
1	Friuli Italy	6.5	1976	15.0	C	TMZ000	0.35	22	2.77
2	Duzce Turkey	7.1	1999	12.0	D	BOL000	0.73	56	0.99
3	Superstition Hills	6.5	1987	11.2	D	B-POE270	0.45	36	1.87
4	Superstition Hills	6.5	1987	11.2	D	B-POE360	0.30	33	1.97
5	Chi-Chi Taiwan	7.6	1999	10.0	D	E-W	0.35	71	1.33
6	Chi-Chi Taiwan	7.6	1999	10.0	D	N-S	0.44	115	0.84
7	Landers	7.3	1992	19.7	D	CLW-LN	0.28	26	2.54
8	Imperial Valley	6.5	1979	22.0	D	H-DLT262	0.24	26	1.90
9	Imperial Valley	6.5	1979	22.0	D	H-DLT352	0.35	33	1.28
10	Imperial Valley	6.5	1979	12.5	D	H-E11230	0.38	42	2.06
11	Northridge	6.7	1994	9.4	D	MUL279	0.52	63	0.71
12	Superstition Hills	6.5	1987	18.2	D	ICC000	0.36	46	1.42
13	Loma Prieta	6.9	1989	12.2	D	G03090	0.37	45	1.40
14	Kocaeli Turkey	7.5	1999	13.6	D	DZC180	0.31	59	1.53
15	Kocaeli Turkey	7.5	1999	13.6	D	DZC270	0.36	46	0.93
16	Cape Mendocino	7.0	1992	7.9	D	RIO270	0.39	44	1.27
17	Kobe Japan	6.9	1995	19.1	D	SHI090	0.21	28	1.66
18	Landers	7.3	1992	23.6	D	YER270	0.24	51	1.24

[a]Peak ground acceleration (PGA) and peak ground velocity (PGV) for original earthquake ground motion records

[b]SF: Scale Factor to match design spectral accelerations over period range $T \in [0.6, 2.0]$ seconds

TABLE 5. Statistics of seismic responses for twelve-story buildings.

Case	Floor Total Acceleration		Connection Force		Connection Deformation		LFRS Shear[a]		LFRS Drift		GLRS Shear		GLRS Drift	
	μ	$\frac{\sigma}{\mu}$	μ	$\frac{\sigma}{\mu}$	μ	$\frac{\sigma}{\mu}$	μ	$\frac{\sigma}{\mu}$	μ	$\frac{\sigma}{\mu}$	μ	$\frac{\sigma}{\mu}$	μ	$\frac{\sigma}{\mu}$
[−]	[g]	[−]	[kN]	[−]	[mm]	[−]	[kN]	[−]	[rad]	[−]	[kN]	[−]	[rad]	[−]
RE	1.52	50%	8986	50%	0	N/A[b]	33281	41%	0.013	21%	1704	18%	0.013	21%
F_{L1-1}	0.65	19%	2532	10%	121	26%	17026	10%	0.010	18%	1558	26%	0.019	18%
F_{L1-2}	0.67	18%	2466	11%	163	22%	15077	9%	0.008	17%	1562	25%	0.020	18%
R_{DC} = 0.8	0.99	6%	5699	5%	14	70%	23927	10%	0.012	20%	1627	19%	0.013	17%
R_{DC} = 1.0	0.82	5%	4641	2%	17	64%	22265	9%	0.012	20%	1664	19%	0.013	18%
R_{DC} = 1.5	0.63	20%	3201	2%	28	39%	18887	8%	0.011	20%	1615	20%	0.012	20%
R_{DC} = 2.0	0.60	25%	2632	5%	54	31%	16737	9%	0.010	17%	1589	22%	0.013	24%
R_{DC} = 2.5	0.61	23%	2383	7%	77	24%	15167	12%	0.009	17%	1561	20%	0.013	20%
R_{DC} = 3.0	0.61	23%	2198	9%	91	25%	14524	11%	0.008	19%	1597	21%	0.012	17%

[a]Design base shear from ASCE/SEI 7 equivalent lateral force procedure is 7835 kN.

μ is the mean value of the maximum peak floor or story responses over the set of ground motions.

σ is the standard deviation value of the maximum peak floor or story responses over the set of ground motions.

$\frac{\sigma}{\mu}$ is the coefficient of variation.

[b]The deformation of rigid connection does not vary and it is essentially zero.

List of Figures

1 Schematic overview of building with planar shear walls and force-limiting deformable connections and schematic of friction device (Tsampras et al. 2018). 35

2 Design acceleration coefficient variation for buildings with (a) 2 or less floors and (b) 3 or more floors. 36

3 Path of seismic-induced horizontal forces. 37

4 (a) C_{Lx} acceleration coefficient. (b) Deformable connection design forces F_{Lx}. (c) LFRS free body diagram subjected to connection design forces F_{Lx}. 38

5 (a) Typical example building floor plan. (b) Schematic of typical example building numerical model. (c) Typical deformable connection force-deformation response. (d) Typical LFRS base hinge moment-rotation response. 39

6 Limiting force values for four-story, eight-story, and twelve-story buildings. 40

7 Pseudo acceleration response spectra for 18 ground motions, median pseudo acceleration spectrum, and design response spectrum for 5% damping. 41

8 Seismic response results for twelve-story buildings. 42

9 Seismic response results for eight-story and four-story buildings. 43

10 Variation of μ_{FLx} (Row 1), μ_{FLx}/μ_{FL1-1} (Row 2), and μ_{FLx}/μ_{RE} (Row 3) with respect to R_{DC} value and number of building stories. 44

11 (a) Earthquake ground acceleration time history (EQ1). (b) EQ1 response spectrum and ASCE/SEI 7 design response spectrum for 5% damping ratio. (c) through (h) First mode and second mode periods for twelve-story building models with RE connections and deformable connections designed for F_{Lx} with $R_{DC} = 3.0,\ 2.0,\ 0.8$ subjected to EQ1. (i) through (n) twelfth-floor and tenth-floor total acceleration time histories of twelve-story building models with RE connections and with deformable connections designed for F_{Lx} with $R_{DC} = 3.0,\ 2.0,\ 0.8$ subjected to EQ1. 45

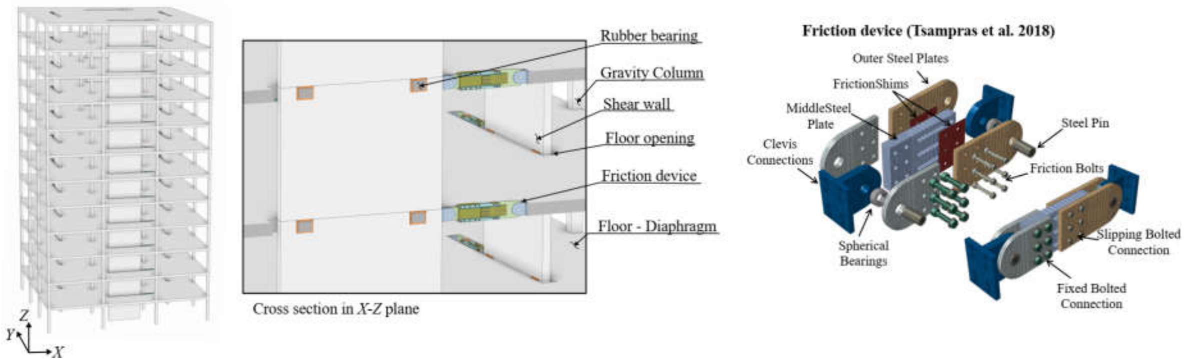

Fig. 1. Schematic overview of building with planar shear walls and force-limiting deformable connections and schematic of friction device (Tsampras et al. 2018).

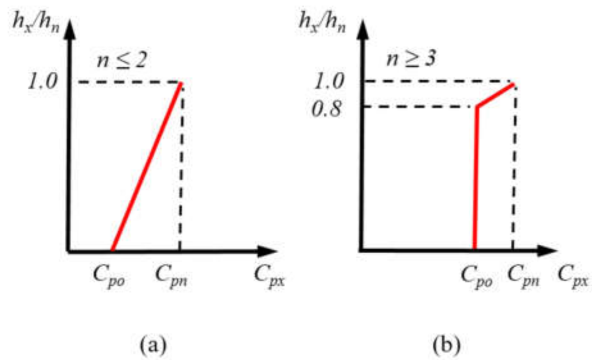

Fig. 2. Design acceleration coefficient variation for buildings with (a) 2 or less floors and (b) 3 or more floors.

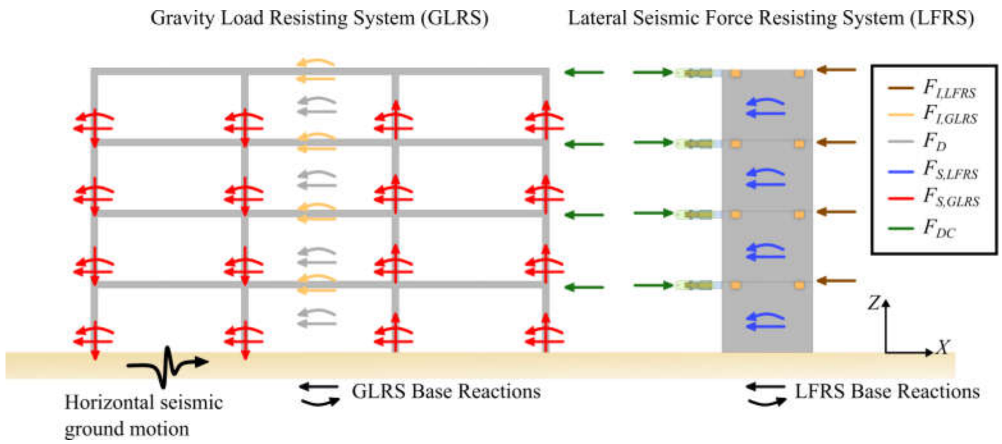

Fig. 3. Path of seismic-induced horizontal forces.

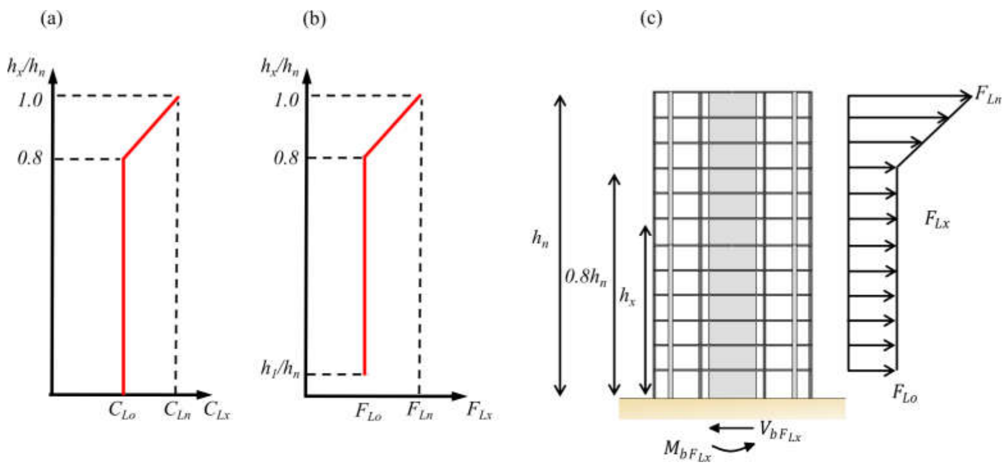

Fig. 4. (a) C_{Lx} acceleration coefficient. (b) Deformable connection design forces F_{Lx}. (c) LFRS free body diagram subjected to connection design forces F_{Lx}.

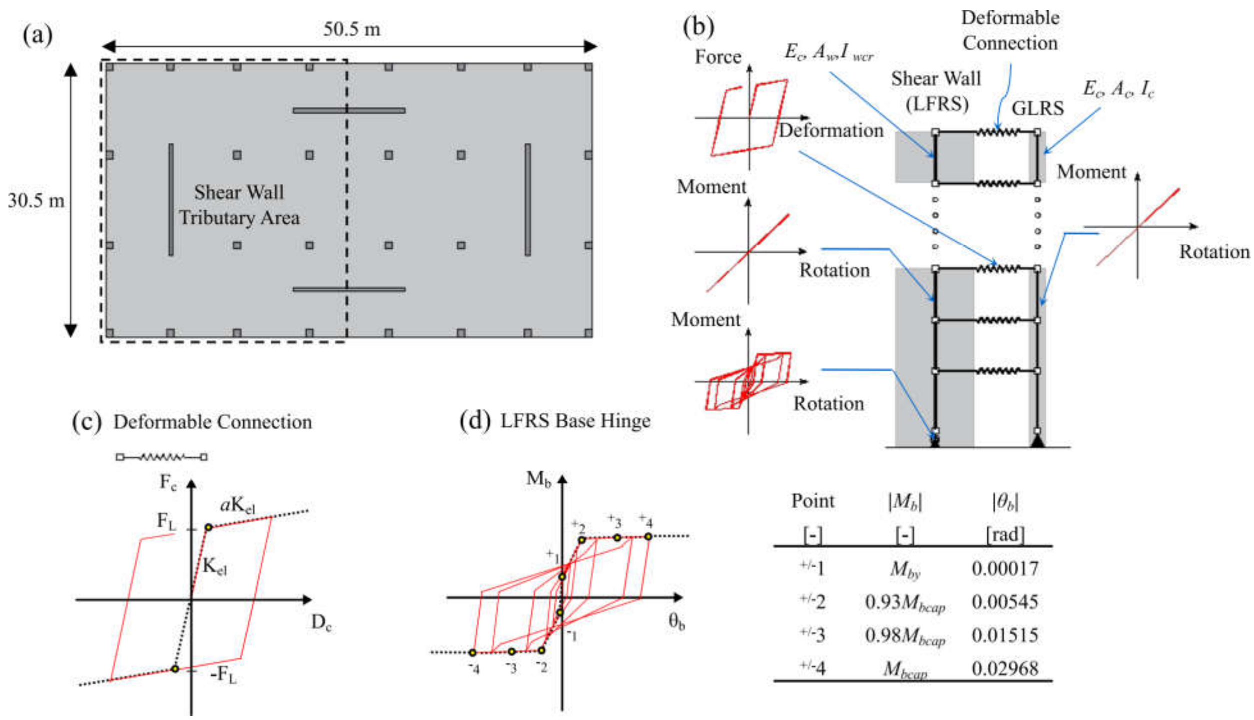

Point	$\lvert M_b \rvert$	$\lvert \theta_b \rvert$
[-]	[-]	[rad]
+/-1	M_{by}	0.00017
+/-2	$0.93M_{bcap}$	0.00545
+/-3	$0.98M_{bcap}$	0.01515
+/-4	M_{bcap}	0.02968

Fig. 5. (a) Typical example building floor plan. (b) Schematic of typical example building numerical model. (c) Typical deformable connection force-deformation response. (d) Typical LFRS base hinge moment-rotation response.

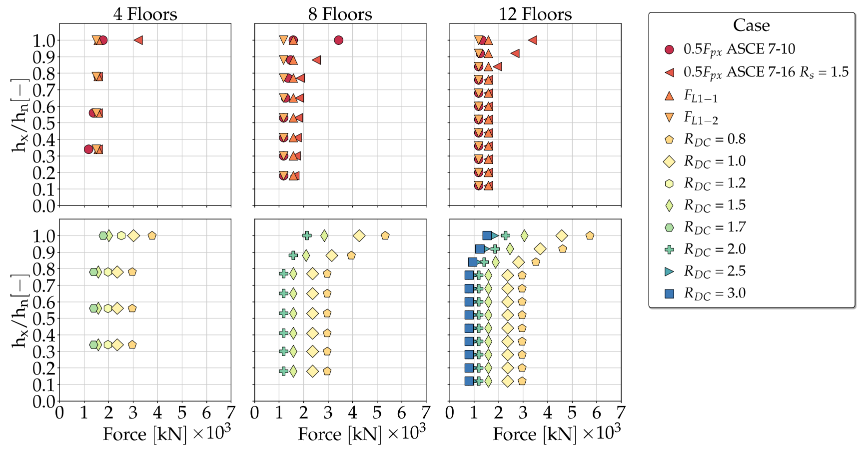

Fig. 6. Limiting force values for four-story, eight-story, and twelve-story buildings.

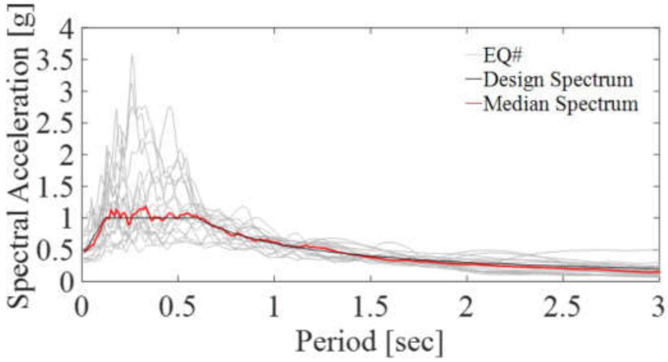

Fig. 7. Pseudo acceleration response spectra for 18 ground motions, median pseudo acceleration spectrum, and design response spectrum for 5% damping.

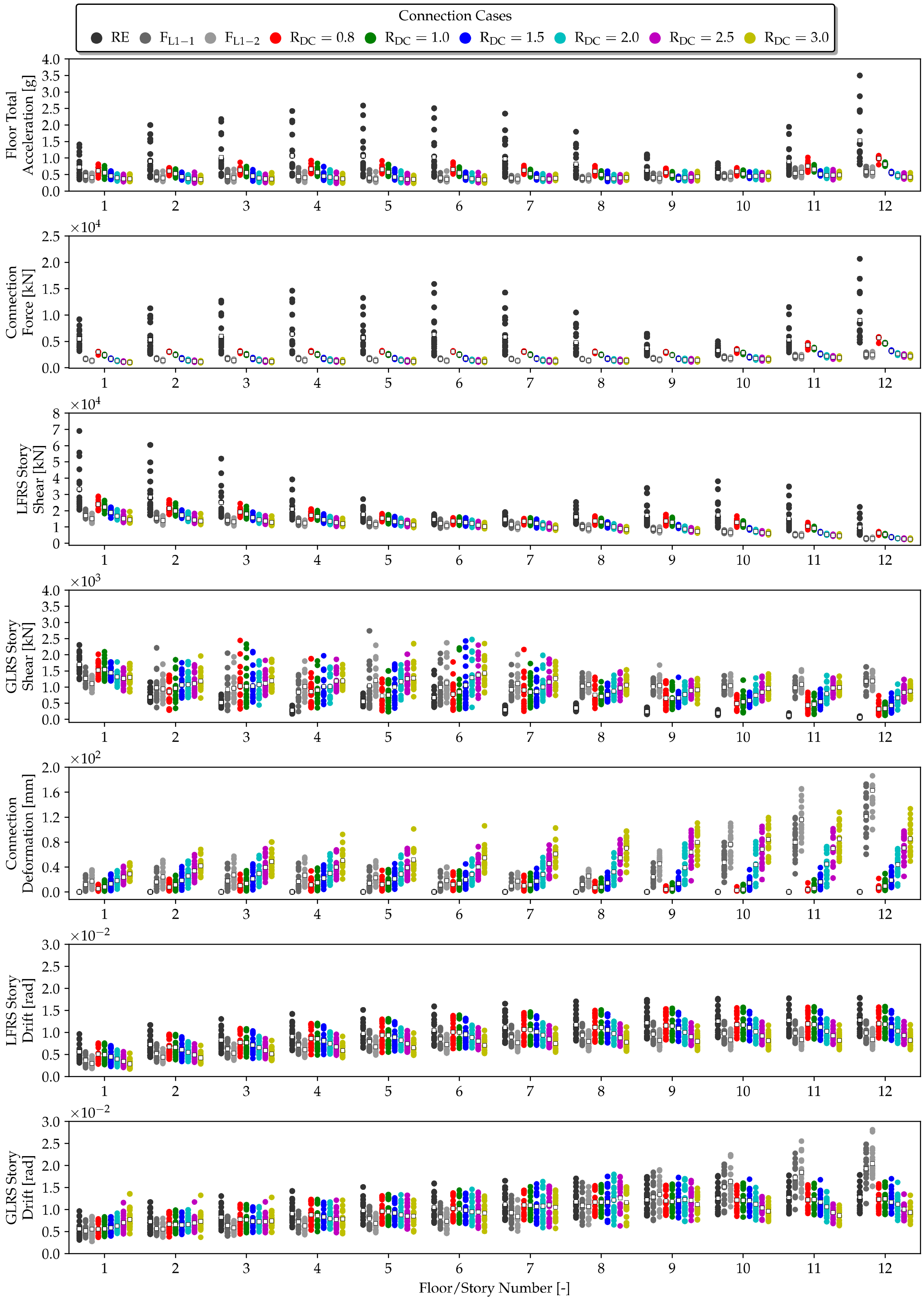

Fig. 8. Seismic response results for twelve-story buildings.

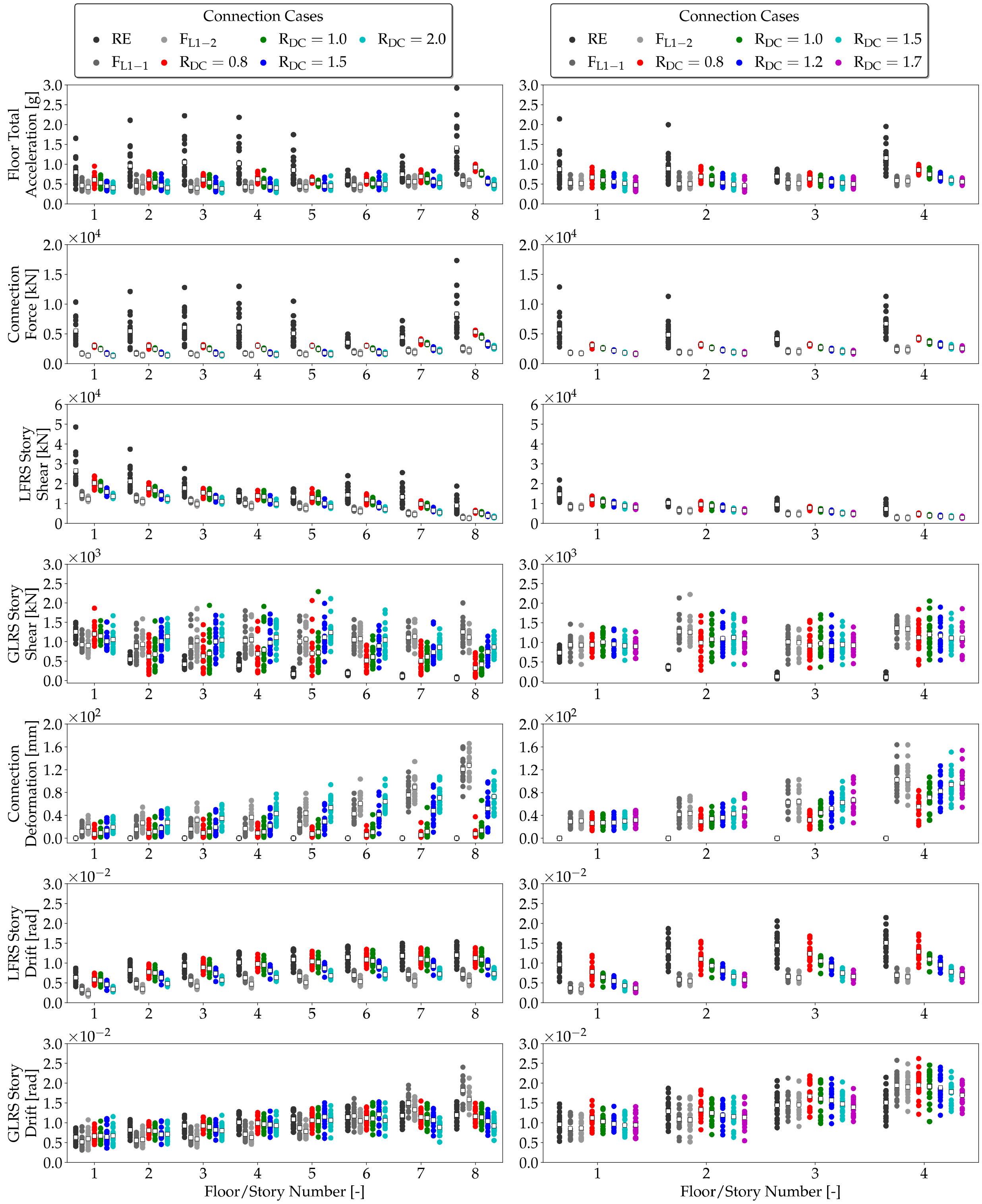

Fig. 9. Seismic response results for eight-story and four-story buildings.

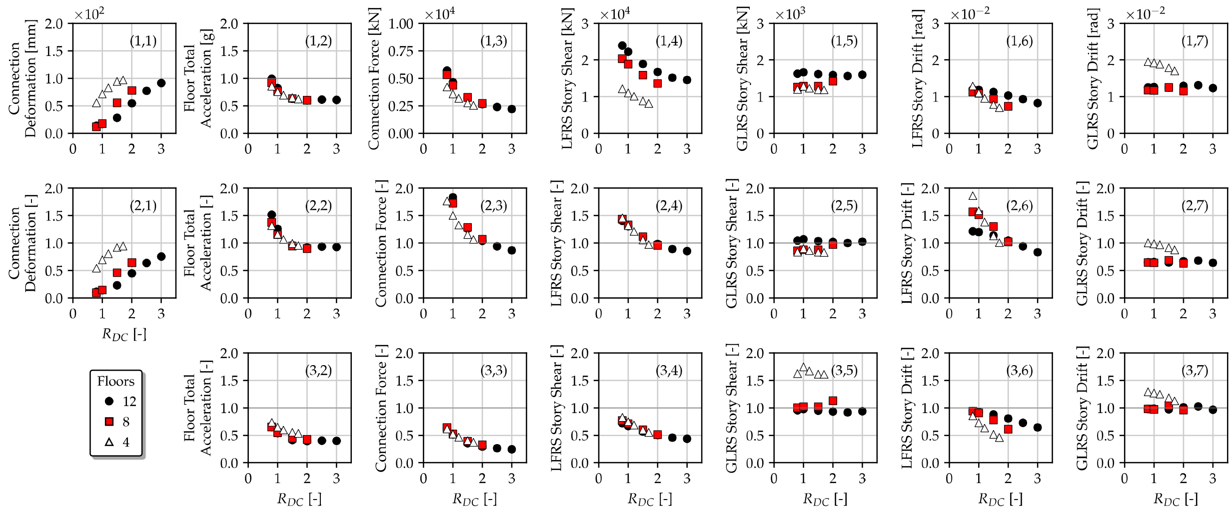

Fig. 10. Variation of μ_{FLx} (Row 1), μ_{FLx}/μ_{FL1-1} (Row 2), and μ_{FLx}/μ_{RE} (Row 3) with respect to R_{DC} value and number of building stories.

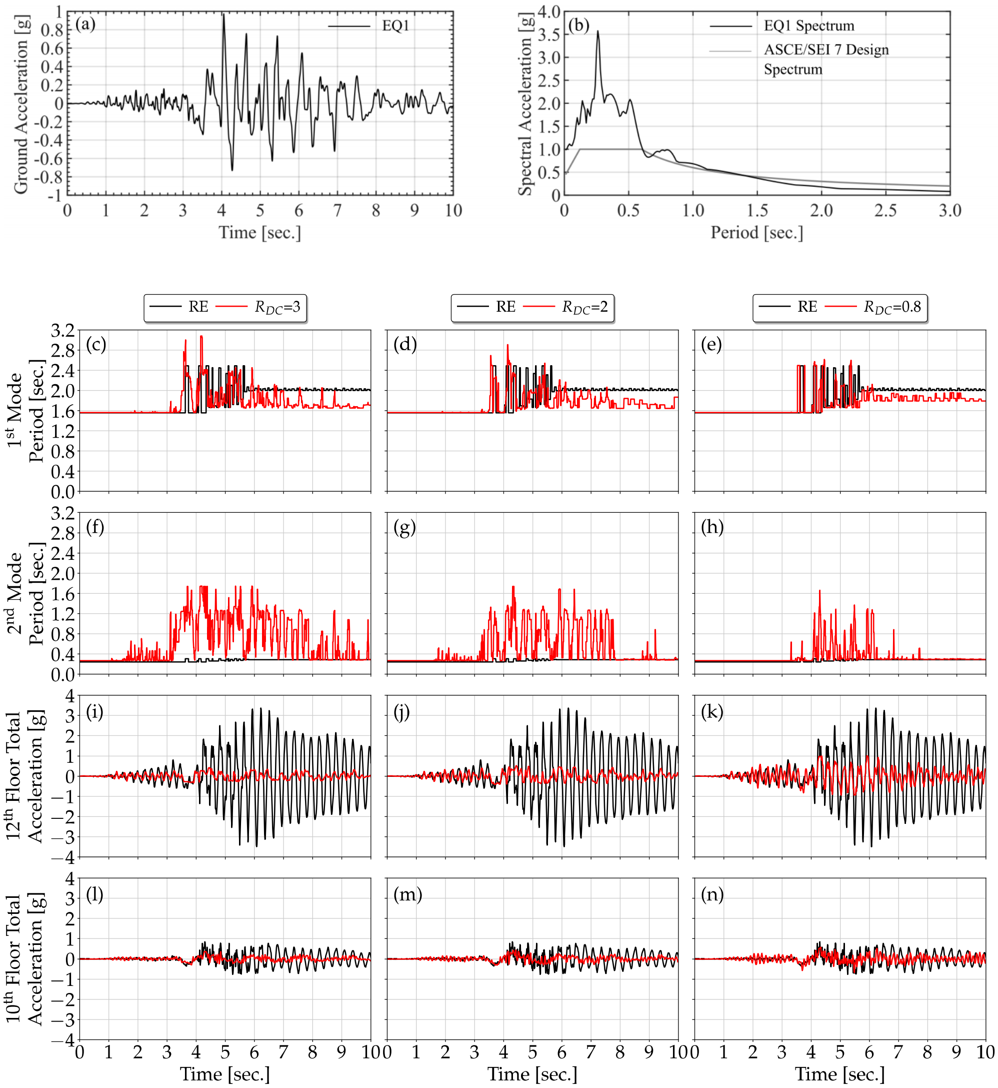

Fig. 11. (a) Earthquake ground acceleration time history (EQ1). (b) EQ1 response spectrum and ASCE/SEI 7 design response spectrum for 5% damping ratio. (c) through (h) First mode and second mode periods for twelve-story building models with RE connections and deformable connections designed for F_{Lx} with $R_{DC} = 3.0,\ 2.0,\ 0.8$ subjected to EQ1. (i) through (n) twelfth-floor and tenth-floor total acceleration time histories of twelve-story building models with RE connections and with deformable connections designed for F_{Lx} with $R_{DC} = 3.0,\ 2.0,\ 0.8$ subjected to EQ1.